

6. A. M. Shams El Din and F. M. Abd El Wahab, *Electrochim. Acta*, **9**, 883 (1964).
7. M. Pugh, L. M. Warner, and D. R. Gabe, *Corros. Sci.*, **7**, 807 (1967).
8. N. A. Hampson and N. E. Spencer, *Brit. Corros. J.*, **3**, 1 (1968).
9. D. R. Gabe and P. Sripatr, *Trans. Inst. Met.*, **51**, 141 (1973).
10. B. N. Stirrup and N. A. Hampson, *J. Electroanal. Chem.*, **67**, 45 (1976).
11. H. Hansen and K. Anderko, "Constitution of Binary Alloys," McGraw-Hill Book Co., Inc., New York, Toronto, London (1958).
12. R. C. Dorward, *Met. Trans.*, **7A**, 308 (1976).
13. H. Ichinose and Y. Ishida, *Scr. Metall.*, **19**, 5 (1985).
14. T. Dickinson and S. Lotfi, *Electrochim. Acta*, **23**, 513 (1978).
15. O. R. Brown and J. S. Whitley, *ibid.*, **32**, 545 (1987).

The Characterization of Electron Cyclotron Resonance Plasma Deposited Silicon Nitride and Silicon Oxide Films

Son Van Nguyen* and Kevin Albaugh*

IBM General Technology Division, Essex Junction, Vermont 05452

ABSTRACT

The physical and bonding properties of electron cyclotron resonance (ECR) plasma-deposited silicon nitride and oxide films deposited in many commercial ECR deposition systems were analyzed using various analytical techniques. ECR films deposited at room temperature showed better qualities than those of plasma-deposited films at higher temperature (350°C). The oxide film qualities are almost comparable to thermal CVD films. However, the nitride film qualities are slightly poorer. For both films, the step coverage is very nonconformal, and sidewall films are much more porous under most deposition conditions. This is due to the anisotropic ion bombardment properties of ECR processing. RF biasing can reduce this effect, fill shallow trenches and planarize the surface structure with appropriate processing conditions.

Low-temperature, plasma-deposited silicon nitride and oxide films are excellent materials that can be used for final passivation layers, and interlevel dielectric films, for very large-scale integrated circuit fabrication (1). Generally, the deposition substrate temperature must be 300°C or higher to obtain good quality films. For ultra-large scale integrated (ULSI) circuit fabrication, better interlevel dielectric films with lower hydrogen concentration are needed. In recent reports (2-3), silicon nitride and oxide films deposited by ECR plasma processing were found to have lower hydrogen concentrations and other promising physical properties. In this paper, we discuss a systematic study of the physical and chemical properties of ECR plasma silicon nitride and oxide films deposited at room (25°C) and elevated (300°C) temperature, and we compare these properties with those of thermal and plasma chemical vapor deposited (CVD) films. The analysis will be focused mostly on low substrate temperature (25°C) films, since low temperature is one of the advantages of the ECR deposition process.

Experimental

ECR plasma silicon nitride oxide films were deposited in various commercial ECR deposition systems with configurations similar to those described in Refs. (2-6). Silane and nitrogen, or silane and oxygen, were used as reactant gases for silicon nitride and oxide films, respectively. In some cases, nitrous oxide gas was also used as the reactant gas for silicon oxide films. Both films were deposited at 25°C or 300°C over bare silicon wafers and wafers with trench structures of various dimensions. In some cases RF bias was applied at the deposition electrode. Overall deposition condition ranges are indicated in Table I in which silicon oxide and nitride films with different refractive indexes can be deposited. The film's physical and bonding properties were analyzed using ellipsometry; Auger, Fourier transform infrared (FTIR), and x-ray photoelectron spectroscopies; transmission electron microscopy; buffered HF etching; and nuclear reaction analysis, to determine the hydrogen concentration.

The solution (7:4:1 buffered HF) for wet etching was prepared by mixing 7 parts (in volume) of HNO₃ with 4 parts of H₂O and 1 part of buffered HF. The one part buffered HF solution was prepared by mixing 10 parts of NH₄F and 1

part HF (in volume). The etch solution temperature was maintained constantly at 25°C during the etch process.

The film thickness and refractive index were measured using a He-Ne laser ellipsometer (wavelength = 632.8 nm). Fourier transform infrared studies were performed with 500 nm films deposited on bare silicon substrate. Auger analysis for compositional depth profiles was performed with 50-100 nm films on silicon substrates using a Physical Electronic Auger spectrometer. The films were sputtered by 1.5 keV Ar⁺ ions at 30s intervals with rastered mode on 100 square micron spot size to determine the composition with depth. To reduce the inhomogenous sputtering effect, the ion beam was rastered for all sputter cleaning processes. The silicon LVV, oxygen KLL, and all N(E) data were taken from double-pass CMA. The concentration of oxygen and nitrogen were determined by normalizing to thermal SiO₂ [O = 66.7 atom percent (a/o)] and CVD is Si₃N₄ (n = 2.01, N = 57 a/o). The detection limit of this equipment is about 1 a/o. The X-ray photoelectron techniques were used to analyze the surface composition of the as-deposited films. The photoemission spectra were obtained with a Hewlett-Packard instrument (Model 5950B) that uses an aluminum K-alpha x-ray source with a monochro-

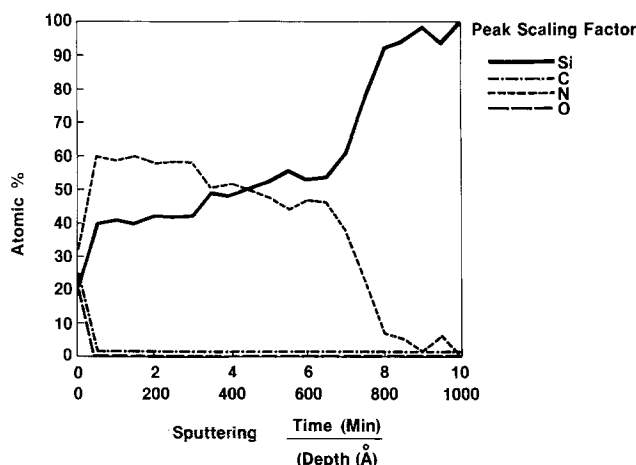


Fig. 1. Typical Auger depth profiles of ECR plasma silicon nitride films deposited at 20°C and 300W RF microwave power.

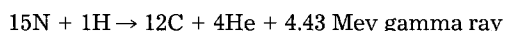
*Electrochemical Society Active Member.

Table I. Typical deposition conditions of ECR films at 25°C

Films	Gas (SCCM)	Pressure (m Torr)	Power (W)	Magnetic Field	Refractive Index	Typical Auger Composition
Silicon Nitride	SiH ₄ (6-15 SCCM)	0.4-1.4	300-500	B = 875 Gauss	1.97-2.15	Si-Rich Nitride SiN _x
	N ₂ (10-30 SCCM)			17 Amp 100 V		x = 0.9-1.3 Poor Depth Profile Uniformity
Silicon Oxide	SiH ₄ (10-15 SCCM)	0.9	300-500	B = 875 Gauss	1.47-1.49	Good Uniformity and Stoichiometry
	O ₂ (6-30 SCCM)			17 Amp 100 V		SiO _{1.9}

mator. The atomic compositions were calculated from the integrated areas of these spectra using a Scofield table as reference (7) and clean, thermally grown silicon oxide films as calibration. Survey spectra were obtained for all films to assess impurities and irregularities.

Hydrogen depth profiling by nuclear reaction analysis was performed on as-deposited ECR silicon nitride and oxide films using the nuclear accelerator equipment at the State University of New York at Albany. The ¹⁵N hydrogen depth profiling is a high precision technique for measuring concentration profiles of hydrogen in solids (8) using the nuclear reaction



In this reaction, the amount of gamma ray emission is proportional to the hydrogen concentration in the film bulk. It should be noted that the nuclear reaction analysis technique determines both bonded (Si-H, N-H, . . . , etc.) and trapped hydrogen (molecular or atomic) in the films without distinguishing the bonding structure. Therefore, the hydrogen concentration result obtained from this technique may be slightly higher than those of FTIR's measurements, especially for films deposited at low temperature where hydrogen can be trapped readily in the film's bulk.

Plasma and thermal CVD films of comparable thickness deposited on Si wafers at much higher temperatures

(300° and 800°C) were also analyzed and compared with ECR plasma films. Both ECR plasma silicon nitride and oxide films were deposited over silicon trench topography, and their step coverage was analyzed under various process conditions using chemical decoration and transmission and scanning electron micrographic techniques.

Results and Discussion

Ellipsometric measurement of as-deposited silicon nitride and oxide films have refractive indexes in the ranges of 1.98-2.15 and 1.46-1.48, respectively. Figure 1 shows typical Auger depth profiles of silicon nitride films deposited at 25°C and 300W microwave RF power. As discussed above, the concentrations of silicon, oxygen, and nitrogen were determined by normalizing to thermally grown SiO₂ (O = 66.7 a/o) and CVD Si₃N₄ (n = 2.01, N = 57 a/o). In most cases, the nitride films deposited at 25°C have poorer depth profile uniformity than those deposited at or higher than 300°C. All the films with refractive indexes of 1.98-2.15 have higher silicon content than the 43 a/o stoichiometric composition of Si₃N₄. This result is consistent with those obtained for plasma deposited silicon nitride films; films with refractive index equal to or above 2.0 are actually silicon-rich silicon nitride films (11). For all silicon oxide films,

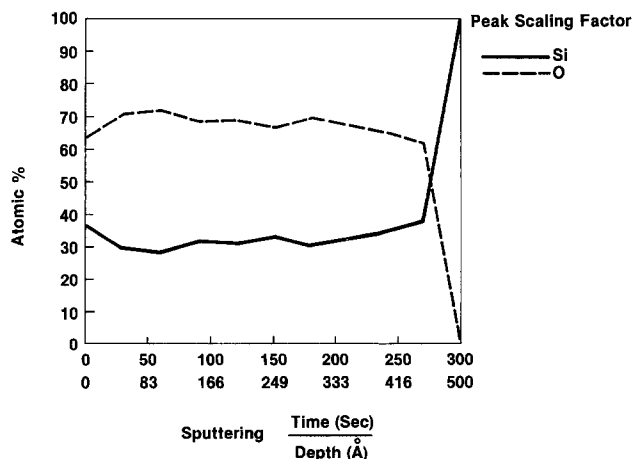


Fig. 2. Typical Auger depth profiles of ECR plasma silicon oxide films deposited at 25°C and 300W RF microwave power.

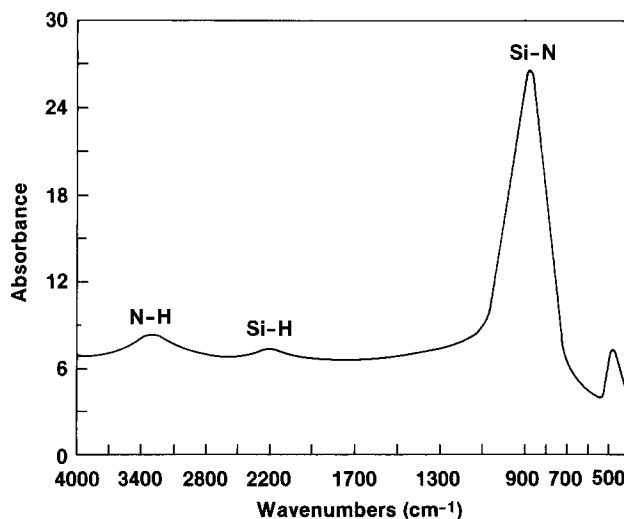


Fig. 3. Typical FTIR spectrum of ECR plasma-deposited silicon nitride films deposited at 25°C and 300W RF power without RF biasing.

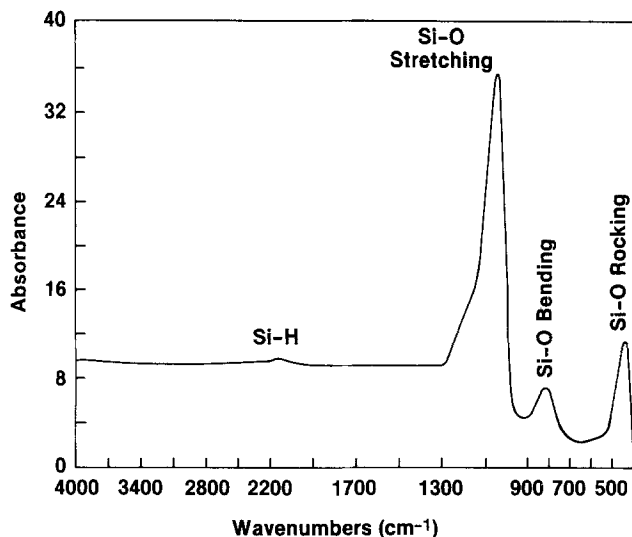


Fig. 4. Typical FTIR spectrum of ECR plasma-deposited silicon oxide films deposited at 25°C and 300W RF power without RF biasing.

the Auger depth profile is much more uniform, with the composition of SiO 1.9 within the ±5% accuracy. Figure 2 shows typical depth profiles of ECR plasma-deposited silicon oxide films deposited at 25°C and 300W microwave RF power.

Figure 3 and 4 show typical FTIR spectra of ECR plasma-deposited silicon nitride and oxide films deposited at room temperature and 300W RF microwave power. The FTIR spectra show the presence of Si—N (880 cm⁻¹), N—H (3340 cm⁻¹), and Si—H (2200 cm⁻¹) bonds in the silicon nitride film. The principal Si—O bonds [1065 (stretching mode), 830 (bending mode), and 450 (rocking mode) cm⁻¹] (10) and Si—H bond (2150 cm⁻¹) were observed in silicon oxide films. It should be noted that oxide films deposited at higher temperature (300°C) and/or RF power (500W), with or without RF biasing, show no sign of Si—H bonding. Table II shows the half-peak width comparison between ECR, thermal and plasma deposited nitride and oxide films. The FTIR spectra of both plasma and thermal silicon nitride and oxide films, used for comparison with ECR plasma-deposited films in this study, have appeared in recent publications (9-12). The vibrational bands half-peak width of the Si—N (880 cm⁻¹) and Si—O (1065 cm⁻¹) modes of the plasma films are normally broader, while those of ECR and thermal films are about the same. This suggests the bonding structure of ECR films is similar to that of thermal films, even at room temperature deposition conditions.

Nuclear reaction analysis shows that the typical hydrogen concentrations in ECR films deposited at room temperature with RF bias are about half of the hydrogen concentration in PECVD films deposited at 300°C. Representative hydrogen depth profiles of ECR, thermal

Table II. FTIR bonding analysis of ECR, thermal and plasma CVD films

Film Type	SiN / SiO Band Position (cm ⁻¹)	Peak Width (cm ⁻¹)	Film Refractive Index (N)	Deposition Temperature (°C)
ECR SiO ₂	1065	110	1.476	25
ECR SiO ₂	1080	110	1.46	300
PECVD SiO ₂	1050	130-230*	1.47	300
LPCVD SiO ₂	1090	110	1.46	800
ECR Si ₃ N ₄	865	210	2.15	25
ECR Si ₃ N ₄	870	220	1.99	300
LPCVD Si ₃ N ₄	870	215	2.00	800
Plasma Si ₃ N ₄	900	240	2.00	350
Plasma Si ₃ N ₄	895	250	1.97	300

* Depending on deposition conditions such as power, flow rate, gas composition. (Our data and references 9-12)

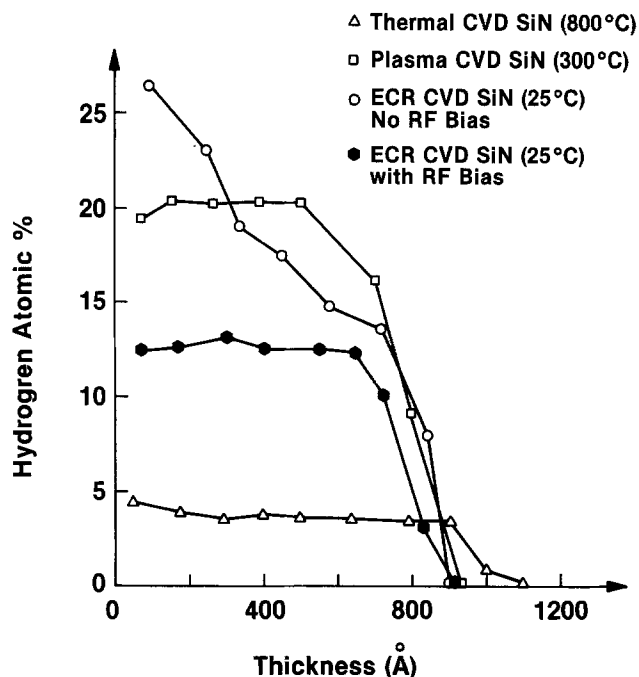


Fig. 5. Hydrogen depth profiles of ECR, thermal and plasma CVD SiN films deposited under various conditions.

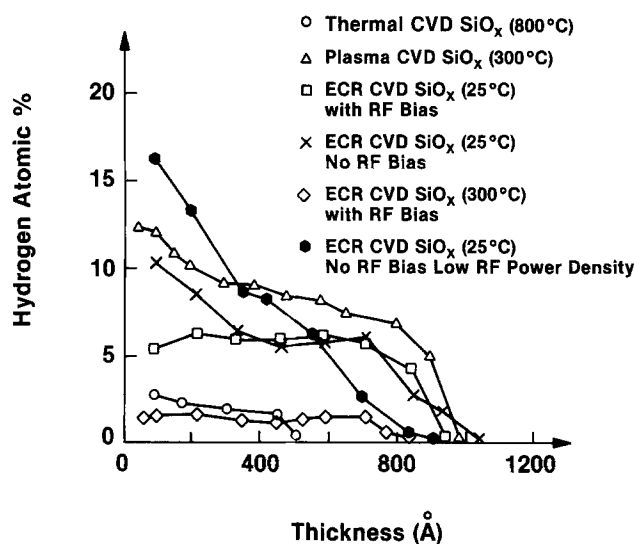


Fig. 6. Hydrogen depth profiles of ECR, thermal and plasma CVD SiO_x films deposited under various conditions.

and plasma CVD silicon nitride and oxide films deposited under different conditions are shown in Fig. 5 and 6. It should be noted that the hydrogen concentrations obtained by this analysis are slightly higher than those tabulated from FTIR Si—H and N—H absorption bands, especially for films deposited at room temperature. For example, the hydrogen concentration of ECR silicon nitride films deposited at room temperature with RF biasing is about 12-13 a/o from the NRA results, and the hydrogen concentration of the same sample tabulated from FTIR data is around 10 a/o. This difference is probably due to trapped hydrogen in the ECR films and the accuracy of both measurement methods. Furthermore, this also suggested that a significant amount of trapped hydrogen existed in ECR films deposited at room temperature.

In general, ECR films deposited with RF bias (at room temperature) tend to have better hydrogen depth profile uniformity and much lower hydrogen concentrations, especially in case of silicon nitride. Increased RF power density and/or substrate temperature also reduces the hydrogen concentration and improves the hydrogen depth profile uniformity significantly, as shown in Fig. 6. This is

Table III. Typical hydrogen content in ECR film vs. 7:4:1 buffer HF solution etching

	Film	Atomic % of Hydrogen	Etch Rate (Å / Min)
PECVD (300°C)	Nitride	20-24	~200
	Oxide	9-12	~1000
CVD (800°C)	Nitride	1.5-2.5	~10
	Oxide	1-2	~50-200
ECR (25°C) 300W	Nitride	15-27 (No RF Bias) 13-15 (With RF Bias)	~100-150 ~50-80
	Oxide	4-6 (With RF Bias) 5-10 (No RF Bias)	~270 ~300-350
ECR (300°C) 500W	Oxide	1-1.5 (With RF Bias)	~50-100

Table IV. X-Ray photoelectron surface analysis of ECR plasma films surface compositions (10-20Å)

	Atomic %				Form
	Si	O	N	Contaminant (Carbon)	
As-Deposited					
Oxide	38	62	..	13	SiO _{1.6}
Nitride	46	30	24	12	Si ₄ N _{2.1} O _{2.6}
After 2 Sec Etching in BHF (Room Temp)					
Oxide	37	63	..	8	SiO _{1.7}
Nitride	55	4	41	13	Si ₄ N ₃ O _{0.3}

Note: Si + N + O = 100%

Si₄N₃ Composition is Normally Observed Surface State of LPCVD Silicon Nitride

due to enhanced ion bombardment on film surfaces with RF bias and increased surface reaction rates with increased temperature, which lower the hydrogen concentration and increase the film's density, as discussed by Hirao (5, 14) and Dun *et al.* (13). At room temperature and similar deposition conditions, hydrogen depth profiles of the ECR oxide films are generally more uniform, and the hydrogen concentration is much lower, than in nitride films. In fact, at 300°C and with RF bias, the hydrogen concentrations in oxide films are even lower than those of thermal CVD films, and are approaching the hydrogen concentration level of thermally grown oxide films

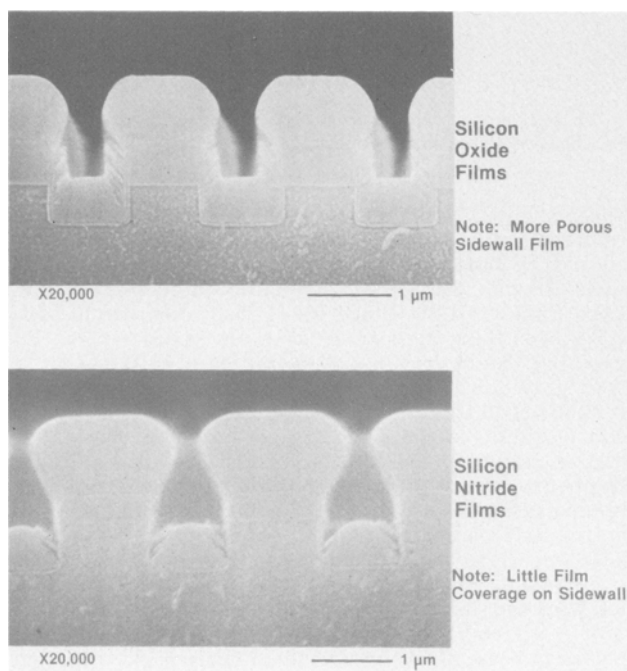


Fig. 7. Step coverage properties of ECR CVD oxide and nitride films deposited without RF bias at room temperature.

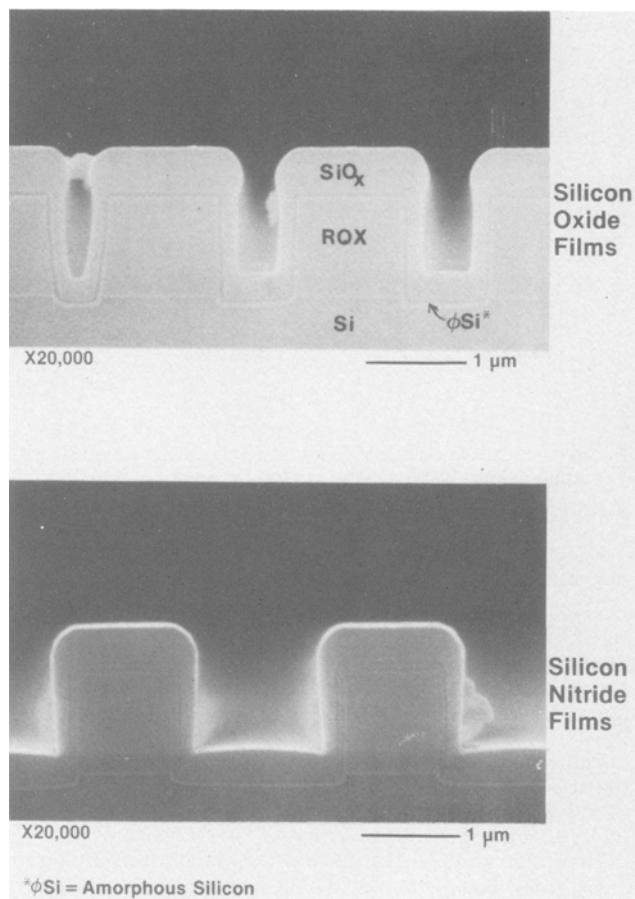


Fig. 8. Step coverage properties of ECR CVD silicon oxide and nitride films deposited without RF bias at 400°C.

(around 0.4 a/o for films grown in wet ambient). However, the ECR films deposited at room temperature still have much higher hydrogen contents than those of thermal CVD films even with RF biasing (Fig. 5, 6 and Table III). It should be noted that the amount of hydrogen observed in our films is near the upper limit of the hydrogen concentration range detected in ECR films reported by Hirao *et al.* (3-5). The overall results indicated that the hydrogen concentrations in ECR films (*i.e.*, the film's physical, chemical, and thermal stability) can be adjusted in a wide range by changing deposition conditions such as RF bias, power density, and substrate temperature, as recently discussed (14).

The 7:4:1 buffered HF etching of ECR, thermal and plasma-deposited CVD films show that the ECR films etch

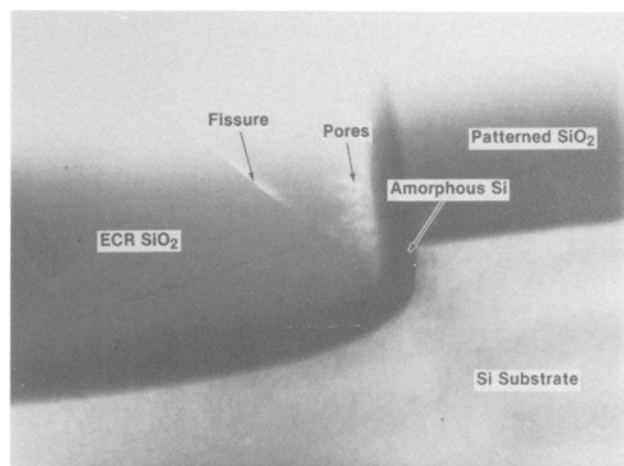


Fig. 9. Lower corner of an ECR SiO₂ filled trench. Note the pores in the oxide along the vertical surface, and the fissure in the oxide where the oxides grown from the bottom and sidewall of the trench meet.

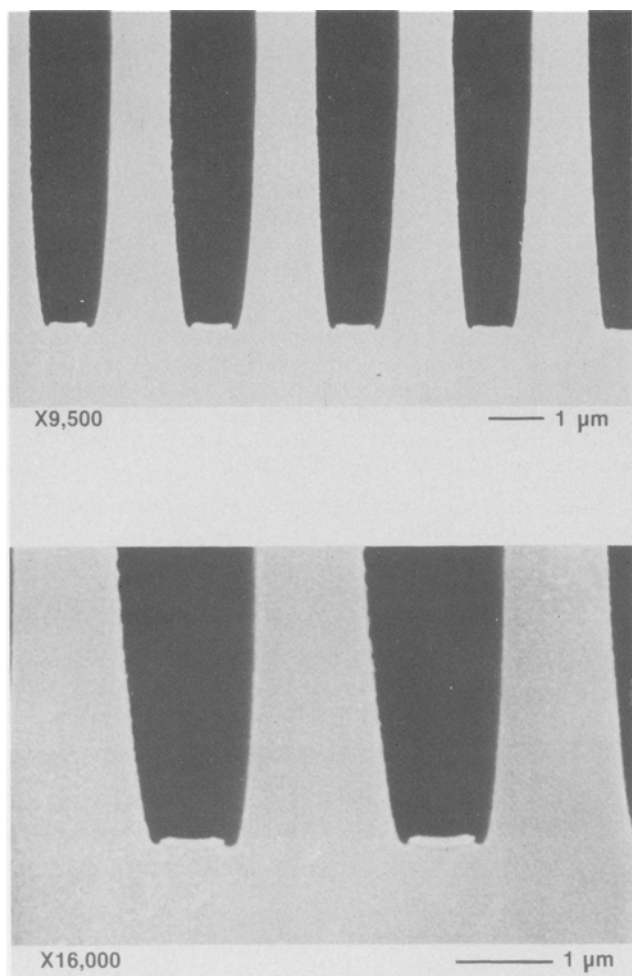


Fig. 10. ECR SiO₂ in trench-relief etch 7:4:1 buffered HF solution. Note oxide layer at trench bottom.

much slower than plasma films, Table III. However, the etch rates of ECR films deposited at room temperature are still significantly faster than thermal films. Oxide films deposited at 300°C and with RF biasing and higher microwave power (500 vs. 300W) have much lower hydrogen con-

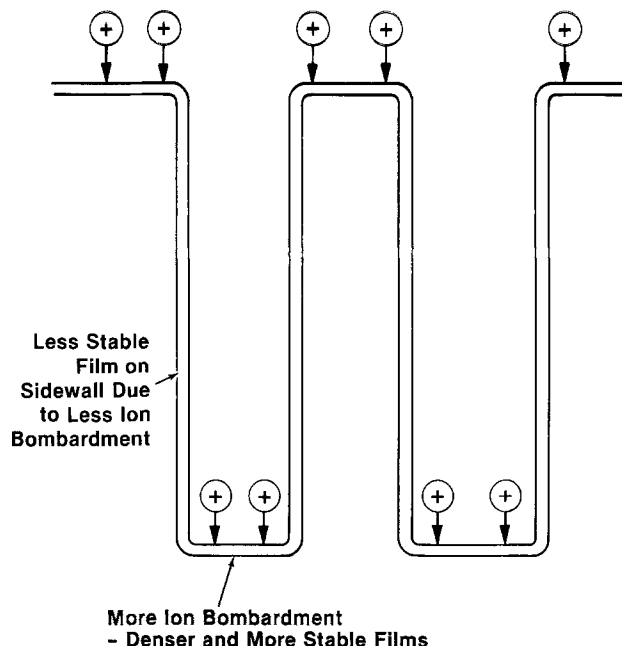


Fig. 11. Intrinsic properties of ECR films deposited on trench and step.

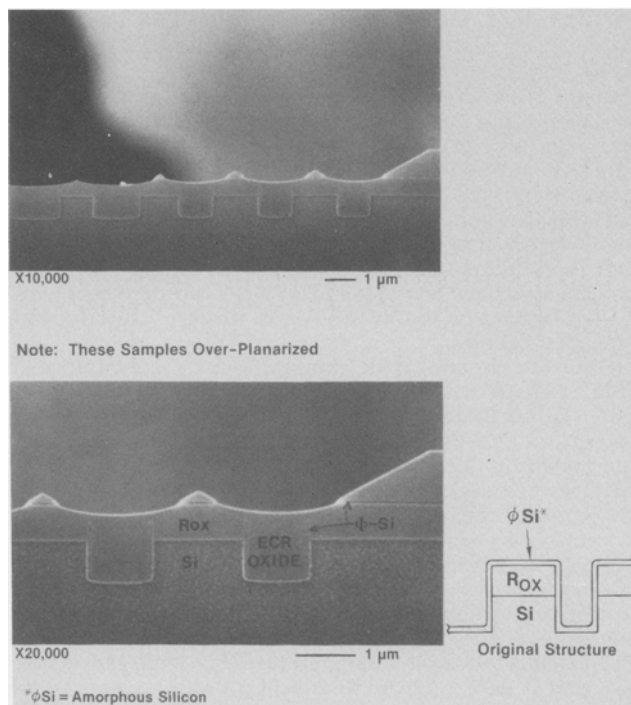


Fig. 12. ECR oxide films deposited with RF bias planarization—excess planarization 420W RF bias.

centration, and the etch rate is almost the same as thermally grown oxide films.

X-ray photoelectron spectroscopy analyses of typical ECR films deposited at room temperature with RF bias show some carbon contamination (8-13 a/o), from exposure in ambient air, in the form of CO₂ and hydrocarbon on both

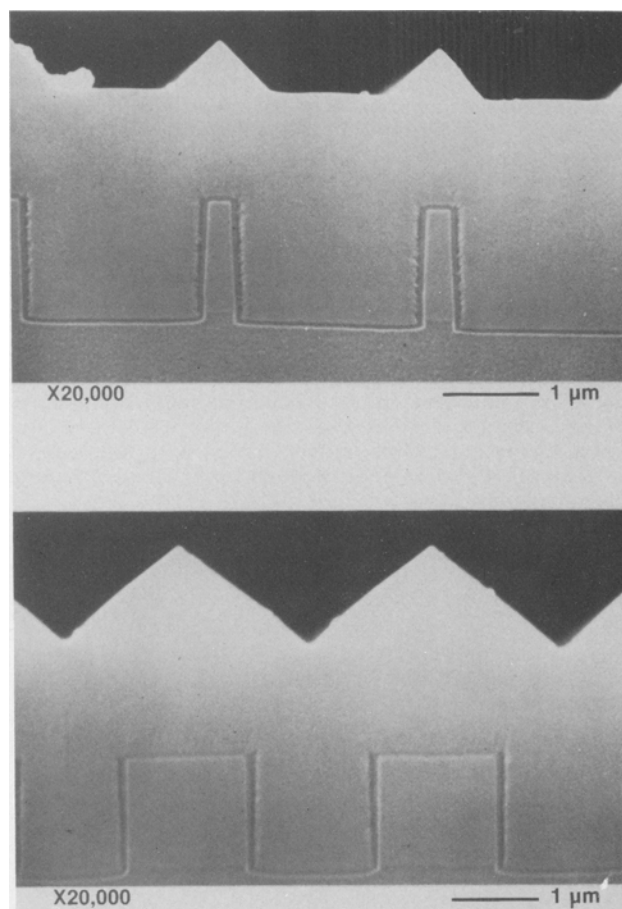


Fig. 13. ECR oxide films deposited with RF bias—200W RF bias

ECR nitride and oxide surfaces (Table IV). The as-deposited surface compositions of both oxide and nitride films have 12-13 at% carbon contamination and a significant amount of oxidized oxygen on nitride films' surface. After wet etching in BHF for 2s, the surface compositions are $\text{SiO}_{1.7}$ for silicon oxide, and $\text{Si}_4\text{N}_3\text{O}_{0.3}$ for silicon nitride films. In addition, significant amounts of carbon contamination in the form of CO_2 and hydrocarbons still exist on surfaces. No significant differences in surface composition were observed between ECR, plasma and thermal nitride and oxide films of similar bulk compositions. This indicates that surface bonding and adhesion properties of ECR CVD films are probably similar to those of thermal and plasma CVD films.

Both nitride and oxide films have very nonconformal step coverage. Films deposited without RF bias have very poor (below 0.4) sidewall coverage, Fig. 7. It can also be seen from Fig. 7 that the vertical sidewall films are more porous and much thinner than films deposited on planar surfaces. In fact, in the case of silicon nitride films, very little coverage was observed on the vertical sidewall. These properties are similar to evaporated films and may be applied for lift-off applications as recently discussed by Shikata *et al.* (15). Films deposited without RF bias but at higher deposition temperatures (400°C) have better step coverage and relatively denser sidewalls compared to those deposited at room temperature (Fig. 8). However, the sidewall coverage is still less than 0.4 and appears to be comparable to the coverage of plasma films deposited at similar conditions. The improvement in sidewall coverage at higher deposition temperature is due to enhanced surface diffusion and deposition of reactive species at higher temperature (13, 16). Transmission electron microscopy shows that sidewall film coatings often have voids, and are more porous and etch much faster in 7:4:1 buffered HF solution, than films deposited on planar surfaces (Fig. 9-10). The film in Fig. 9 was deposited without RF bias during the initial stage of film growth, then with bias for the remainder of the film. The voids occur in the portion deposited without bias, and the fissure occurs during deposition with bias. This is due to the enhanced vertical ion bombardment characteristic of ECR processing (5), as shown in Fig. 11, which densifies films deposited on planar surfaces. As a result, films deposited on planar surfaces will etch more slowly even at deep trench bottoms (Fig. 10).

With RF bias, oxide films can fill shallow trenches as shown in Fig. 12 and 13. This trench-filling characteristic is consistent with the results obtained by Machida (6). However, low RF biasing will cause jagged edges on the planarization surface, Fig. 13, and excess RF biasing can overplanarize and create undesirable structures, Fig. 12. High RF biasing can also cause significant damage to the substrate during the initial trench fill process. In general, the trench structure can be filled with low RF bias condition and the surface can be planarized with higher RF biasing to reduce damage to the substrate. The degree of RF biasing is dependent upon various parameters such as process condition, film type, and substrate structure. Under many conditions, a deep trench with high aspect ratio (depth/width) cannot be filled by ECR silicon oxide and nitride films.

Conclusion

The physical and bonding characteristics of ECR plasma-deposited silicon nitride and oxide films were ana-

lyzed using various analytical techniques. ECR films deposited at room temperature showed better qualities than those of plasma-deposited films at higher temperature (350°C). The oxide film qualities are almost comparable to thermal CVD films; however, the nitride film qualities are slightly poorer. For both films, the step coverage is very nonconformal and sidewall films are much more porous under most deposition conditions. This is due to the anisotropic ion bombardment properties of ECR processing. RF biasing can reduce this effect, fill shallow trenches, and planarize the surface structure with appropriate processing conditions.

Acknowledgments

The authors wish to acknowledge the contribution of K. Furland, S. Fridmann, D. Dicicco, W. Hathaway, G. Devereaux, L. Nesbit, and R. Gleason of IBM, and also Professor W. A. Lanford of State University of New York at Albany in many analyses of ECR films.

Manuscript submitted Oct. 24, 1988; revised manuscript received Feb. 3, 1989.

IBM assisted in meeting the publication costs of this article.

REFERENCES

1. S. V. Nguyen, *J. Vac. Sci. Technol. B*, **4**, 1159 (1986).
2. T. Kikkawa, S. Chikaki, Y. Matsumoto, T. Ueno, and H. Wanatabe, in "Reduced Temperature Processing for VLSI," Vol. 86-5, R. Reif and G. R. Srinivasan, Editors, p. 235, The Electrochemical Society Softbound Proceedings Series, Pennington, NJ (1986).
3. T. Hirao, K. Setsune, M. Kitagawa, T. Kamada, K. Wasa, and T. Izumi, *Jpn. J. Appl. Phys.*, **26**, 2015 (1987).
4. T. Hirao, K. Setsune, M. Kitagawa, T. Kamada, K. Wasa, and T. Izumi, *Jpn. J. Appl. Phys.*, **27**, 30 (1988).
5. T. Hirao, K. Setsune, M. Kitagawa, Y. Manabe, K. Wasa, and S. Kohiki, *Jpn. J. Appl. Phys.*, **26**, L544 (1987).
6. K. Machida and H. Oikawa, *J. Vac. Sci. Technol. B*, **4**, 818 (1986).
7. Scofield Table, *J. Electron. Spectrosc. Relat. Phenom.*, **8**, 129 (1976).
8. W. A. Lanford and M. J. Rand, *J. Appl. Phys.*, **49**, 2473 (1978).
9. P. Pan, L. A. Nesbit, R. W. Douse, and R. T. Gleason, *This Journal*, **132**, 2012 (1985).
10. G. Luvosky, P. D. Richard, D. V. Tsu, S. Y. Lin, and R. J. Markunas, *J. Vac. Sci. Technol. A*, **4**, 681 (1986).
11. S. V. Nguyen and S. Fridmann, *This Journal*, **134**, 2324 (1987).
12. S. V. Nguyen, J. Abernathy, S. Fridmann, and M. Gibson, "Emerging Semiconductor Technology," ASTM STP 960, D. C. Gupta and P. H. Langer, Editors, p. 173, American Society for Testing and Materials (1987).
13. H. Dun, P. Pan, F. R. White, and R. W. Douse, *This Journal*, **133**, 1555 (1981).
14. T. Hirao, K. Setsune, M. Kitagawa, T. Kamada, K. Wasa, A. Matsuda, and K. Takana, *Jpn. J. Appl. Phys.*, **27**, 528 (1988).
15. S. Shikata, H. Hayashi, H. Takashashi, and K. Yoshida, in "Advanced Processing Semiconductor Devices," Pub. 797, pp. 126-129, Society of Photo Instruments Engineers (1987).
16. R. C. Ross and J. L. Vossen, *Appl. Phys. Lett.*, **45**, 239 (1984).